

## Dynamical coefficients for a Josephson vortex in an anisotropic junction

Mark W. Coffey

*Department of Physics, University of Colorado, Boulder, Colorado 80309*

(Received 2 September 1999; revised manuscript received 22 November 1999)

The mass per unit length  $\mu$  and drag coefficient  $\eta$  for a Josephson vortex moving and aligned parallel to the plane of an anisotropic Josephson junction are calculated. The tilt angle between the vortex direction and the crystal uniaxial directions of the superconducting banks is allowed to vary, so that this type of misalignment of the banks is included. These low-field results are suitable for inclusion in the dynamic mobility of Josephson vortices. These dynamical coefficients should be applicable to the description of the intergrain motion of vortices in polycrystals of high- $T_c$  superconductors. The extension of the approach for the regime of relativistic vortex motion is presented.

### INTRODUCTION

The calculation of dynamical coefficients is of importance in describing a wide range of vortex phenomena in superconductors including radio frequency (rf) response,<sup>1,2</sup> entropy and current flow, and quantum tunneling.<sup>3</sup> A suitable function for describing vortex response is the complex-valued dynamic mobility.<sup>4,2,5</sup> The mobility can simultaneously include the effects of inertia, pinning, flux flow, and flux creep. A characterization of the vortex drag coefficient is key to quantifying the dissipation due to vortex motion. Knowledge of the vortex mass is desirable in determining whether to include an inertial term in the equation of motion. The vortex mobility can be written in the limiting case when the viscous drag force vanishes, where inertial effects should be pronounced.<sup>4,5</sup>

Since the discovery of the high- $T_c$  superconductors, several studies have examined the drag coefficient and mass per unit length of Abrikosov vortices within the framework of the anisotropic Ginzburg-Landau (GL) theory.<sup>6,7</sup> This theory is incomplete and remains an active area of investigation. On the other hand, the anisotropic GL theory treats the superconductor as continuous and therefore does not take into account either the intrinsic layered nature of  $\text{CuO}_2$ -based compounds or the polycrystalline nature of many macroscopic samples.

This contribution is directed toward the latter subject. We present dynamical quantities for a Josephson vortex located in the barrier region of an anisotropic Josephson junction. We give results for the vortex drag coefficient and mass per unit length in the low-field limit. That is, in this study vortex interaction is ignored. As for equations governing the gauge invariant phase difference in the presence of effective mass anisotropy, we rely on a recent derivation by Mints and Kogan (MK).<sup>8</sup> The principal results of our study are given in the form of a table, where we include the isotropic results due to Leubwohl and Stephen (LS) (Ref. 9) for comparison.

In this discussion of dynamical coefficients, it is important to account for the nonzero thickness  $d_i$  of the insulating layer in the Josephson junction. In particular, this is necessary in considering the electric field induced by the motion of the vortex. In regard to maintaining  $d_i \neq 0$ , we are thus able to slightly extend the results of MK and an earlier result

of Mints<sup>10</sup> for the lower critical field of an anisotropic junction. Normally this extension is negligible, except for the case of low- $\kappa$  (GL parameter) superconductors. The paper of MK concentrated on finding the Gibbs and Helmholtz free energies and the resulting mechanical torque on parallel lines of Josephson vortices.

Here we assume a Josephson vortex moving at constant velocity parallel to the plane of an anisotropic junction and focus on the induced electric field. This field energy in turn yields both the drag coefficient and the electromagnetic contribution to the vortex mass. We recall that unlike Abrikosov vortices, Josephson vortices lack a core region of suppressed order parameter. Therefore the generally much larger core contribution to the vortex mass is absent for Josephson vortices.<sup>7,11</sup>

For many superconducting junctions, typically  $\lambda \ll \lambda_J$ , where  $\lambda$  is the geometric mean penetration depth and  $\lambda_J$  is the Josephson penetration depth, which in turn influences the relative sizes of the lower critical fields for bulk crystal versus junction penetration. Therefore the flux penetration into twinned crystals begins with nucleation of Josephson vortices at twin planes in superconductors similar to  $\text{YBa}_2\text{Cu}_3\text{O}_{7-\delta}$ . Given this relation between  $\lambda$  and  $\lambda_J$ , it should be experimentally possible to operate in the very low-field regime considered in this paper, where Josephson but not Abrikosov vortices are present.

The discussion proceeds from the simpler geometry of an anisotropic junction with aligned superconducting banks to that with misaligned banks. In these two respective sections, the vortex speed  $v$  is assumed to be much less than  $\bar{c}$ , the speed of light in the junction barrier. The succeeding section considers removing this restriction. Therefore the goal of that examination is to present the key ingredients in performing relativistically consistent calculations.

The flux flow resistivity and corresponding drag coefficient for Josephson vortices aligned and moving parallel to the  $\text{CuO}_2$  planes have been experimentally determined for  $\text{Bi}_2\text{Sr}_2\text{CaCu}_2\text{O}_{8+y}$  ( $\text{Bi}2212$ ).<sup>12</sup> The data come from vortex flow  $I$ - $V$  (current versus voltage) characteristics at 77 K and have been found to be in quantitative agreement with models for vortex motion in layered superconductors.<sup>12,13</sup> The results of this paper may provide a basis for further understanding the role of effective mass anisotropy in such layered models.

For the superconducting stack models, two-dimensional (2D) phase difference solutions are required. For these models, questions concerning the Lorentz invariance of the coupled sine-Gordon equations have arisen.<sup>12</sup> This is a separate topic for future research.

An example of the microwave response of superconducting weak links is given in Ref. 14, where the authors considered the dynamics of vortices in long Josephson junctions subjected to a time-harmonic ac magnetic field. This reference numerically examined a range of applied field strength, whereas this paper is mostly restricted to the very small field limit. On the other hand, Ref. 14 neglected the capacitive term, which is responsible for the second-order time-derivative term in the equation of motion of the phase difference. This term is important in the consideration of wave propagation and relativistic effects. The vortex drag coefficient derived here is related to the damping parameter of Ref. 14 in the limit of small applied field. This paper assumes a steadily propagating Josephson vortex and then finds the lowest order contribution to the dissipation, while the framework of Ref. 14 is appropriate to damped sinusoidal solutions.

Magnetoabsorption microwave resonances observed in Bi2212 (Refs. 15 and 16) are an important source of information for studying the interlayer Josephson coupling in high- $T_c$  superconductors. These experiments allow the interlayer phase coherence to be quantitatively determined in a wide range of magnetic field. An interpretation of the results has been made in terms of a Josephson plasma resonance. However, an alternative explanation<sup>17</sup> invokes a vortex vibration mode, where the vortex inertia is critical.

In addition, the microwave dissipation in Bi2212 has been measured at 10 GHz, as a function of both temperature and magnetic field applied along the  $c$  axis.<sup>18</sup> These various experiments likely involve the diffusive motion of pancake vortices and the dynamics of Josephson strings. Therefore a number of investigations into the appropriate dynamical coefficients for Josephson strings and 2D vortices are called for. This paper is concerned with these quantities for a long Josephson string. Another area where these results may be applicable is in the first-order decoupling transition in a layered organic superconductor.<sup>19</sup>

### ALIGNED BANKS

We first recall some notation of the anisotropic GL theory and then specify the geometry of the junction and Josephson vortex. The penetration depths  $\lambda_i = \lambda \sqrt{m_i}$  in terms of the effective masses  $m_i$  and  $\lambda = (\lambda_1 \lambda_2 \lambda_3)^{1/3} = (\lambda_a^2 \lambda_c)^{1/3}$ . Here, a uniaxial material with  $\lambda_a = \lambda_b$  is assumed. The anisotropy ratio is written as  $k = \sqrt{m_c/m_a} = \lambda_c/\lambda_a$ . For YBCO,  $k \approx 5.5$  and for HgBa<sub>2</sub>Ca<sub>2</sub>Cu<sub>3</sub>O<sub>8+\delta</sub>,  $k \approx 27$ . For the organic superconductor K-(ET)<sub>2</sub>Cu[N(CN)<sub>2</sub>]<sub>2</sub>Br, the axial direction is the  $a$  axis and then  $\sqrt{m_a/m_c} \approx 9$ .

Let the plane of the junction be the  $xz$  plane, with the  $y$  axis coincident with the  $b$  crystal axis. This section assumes a junction of the same anisotropic material in the two banks, which are exactly aligned. We take the convention of Ref. 8 with the vortex along the  $z$  axis and the angle between  $\hat{z}$  and the crystal  $c$  axis denoted by  $\theta$ ; see Fig. 1.

In this instance, the gauge invariant phase difference  $\varphi$

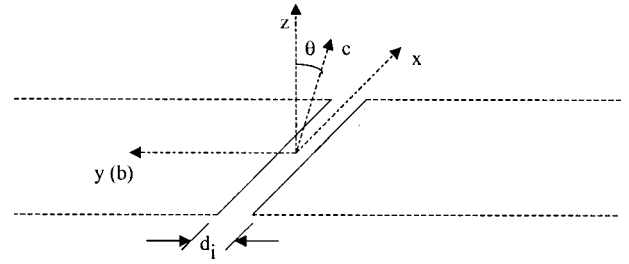


FIG. 1. Geometry of the anisotropic but aligned Josephson junction. The  $xz$  plane is the plane of the junction, which has insulator thickness  $d_i$ . The crystal  $b$  axis is coincident with the  $y$  axis. A Josephson vortex along the  $z$  axis makes an angle  $\theta$  with the crystal  $c$  axis, the uniaxial direction of a high- $T_c$  superconductor. The superconducting banks are described by effective mass tensors  $m_{\alpha\beta}$  and  $\mu_{\alpha\beta}$  with respective eigenvalues  $m_i$ ,  $i=a,b,c$  and  $1/\sqrt{m_j}$ ,  $j=a,c$  where  $m_i$  are the effective masses.

across the junction satisfies the sine-Gordon equation

$$\Lambda_J^2 \varphi'' = \sin \varphi, \quad (1)$$

where  $'$  denotes differentiation with respect to  $x$ ,  $\Lambda_J(\theta) = \lambda_J \sqrt{\mu_{xx}(\theta)}$ ,  $\lambda_J = (c \phi_0 / 16 \pi^2 \lambda J_c)^{1/2}$  is the Josephson penetration depth, and

$$\mu_{xx} = k^{-2/3} \sin^2 \theta + k^{1/3} \cos^2 \theta. \quad (2)$$

Above,  $\phi_0$  is the flux quantum and  $J_c$  is the junction critical current density.

Equation (1) has the single soliton solution

$$\varphi(x) = 4 \tan^{-1} [\exp(x/\Lambda_J)], \quad (3)$$

which we now use to compute the Josephson vortex drag coefficient  $\eta$ . The power dissipated per unit length  $\eta v^2$ , with  $v$  the vortex speed, corresponds to the friction force per unit length  $-\eta v$ . Equating this dissipated power to that arising from Ohmic currents generated in the junction barrier by the induced electric field, we have

$$\eta v^2 = \frac{1}{R'} \left( \frac{\hbar}{2e} \right)^2 \int_{-\infty}^{\infty} \left( \frac{\partial \Delta \gamma(x,t)}{\partial t} \right)^2 dx, \quad (4)$$

where  $R' = \rho_b d_i$  is the contact resistivity. For speeds  $v \ll \bar{c}$ , where  $\bar{c} = c \sqrt{d_i/\epsilon d}$  is the speed of light in the junction, we can take  $\Delta \gamma(x,t) = \varphi(x - vt)$ . In the definition of  $\bar{c}$ ,  $\epsilon = \epsilon_b$  is the dielectric constant of the barrier and  $d = 2\lambda + d_i$  is the magnetic thickness.<sup>4</sup>

By making use of Eq. (3) in Eq. (4) we then find the anisotropy and angular dependence of the drag coefficient,

$$\eta(\theta) = \frac{2 \phi_0^2}{\pi^2 c^2} \frac{1}{R'} \frac{1}{\Lambda_J(\theta)}. \quad (5)$$

In this equation, by Eq. (2), for  $\theta \rightarrow 0$ ,  $\mu_{xx}(0) = k^{1/3}$ , and  $\Lambda_J(0) = \lambda_J k^{1/6}$ , while for  $\theta \rightarrow \pi/2$ ,  $\mu_{xx}(\pi/2) = k^{-2/3}$ , and  $\Lambda_J(\pi/2) = \lambda_J k^{-1/3}$ . Therefore  $\eta(0)/\eta(\pi/2) = k^{-1/2}$ . For  $k \rightarrow 1$ , the isotropic result due to LS is recovered.<sup>9</sup>

The result (5) is valid for sufficiently small resistivity  $\rho_b$ . A quantitative version of this condition may be  $\beta_C = R C \omega_p \ll 1$ , where  $R = \rho_b d_i / A$  is the normal resistance,  $C = \epsilon A / 4 \pi d_i$  is the junction capacitance,  $A$  is the junction area,

and  $\omega_p = \bar{c}/\lambda_b$  is the angular frequency of longitudinal plasma waves in the insulating barrier. Here,  $\beta_C$  is the McCumber-Stewart parameter.<sup>20</sup> When this condition holds, solutions of the time-dependent sine-Gordon equation are ensured to be dominated by wavelike instead of diffusive behavior.

For a general direction of vortex motion, the rate of energy dissipation per length can be written as  $D = \eta_{ij}v_i v_j$  with  $\eta_{ij}$  a viscous drag tensor. We have calculated  $\eta_{xx}$  appropriate to our junction geometry. Then the corresponding flux flow resistivity  $\rho_f$  follows from the expression  $\rho_f = \phi_0 B/c^2 \eta$ , where  $B$  is the averaged magnetic flux density, as

$$\rho_f(\theta) = \frac{\pi^2}{2} \frac{B}{\phi_0} R' \Lambda_J(\theta). \quad (6)$$

Putting the vortex kinetic energy per length equal to the induced electric-field energy per length yields the electromagnetic contribution to the vortex mass per unit length  $\mu$ . This gives, for small vortex velocities,

$$\mu = \frac{\epsilon}{4\pi v^2} \int E^2(\mathbf{x}) d^2x, \quad v \ll \bar{c}, \quad (7)$$

where  $E_y(x, t) = (\hbar/2ed_i) \partial \Delta \gamma(x, t) / \partial t$ . Including relativistic effects, as is done in a succeeding section, we use the expression  $K = (\gamma_v - 1) \mu \bar{c}^2$  for the kinetic energy, where the factor  $\gamma_v = 1/\sqrt{1 - v^2/\bar{c}^2}$ . By using the adiabatic approximation for  $\Delta \gamma(x, t)$  as above, we have

$$\mu = \frac{\epsilon}{4\pi} \left( \frac{\hbar}{2ed_i} \right)^2 d_i \int_{-\infty}^{\infty} \left( \frac{\partial \varphi}{\partial x} \right)^2 dx. \quad (8)$$

Evaluation of the integral using Eq. (3), as above, yields

$$\mu(\theta) = \frac{1}{2\pi^3} \frac{1}{\bar{c}^2} \frac{\phi_0^2}{d\Lambda_J(\theta)}. \quad (9)$$

In the isotropic case  $k=1, \Lambda_J = \lambda_J$ , this result is consistent with that of LS.<sup>9</sup>

The vortex mobility  $\tilde{\mu}_v$  (Refs. 2, 5, and 4) enters the general relation between velocity  $\mathbf{v}$  and driving force  $\mathbf{f}$  as  $\mathbf{v} = \tilde{\mu}_v \mathbf{f}$ . The driving force in the vortex equation of motion may be the Lorentz force, Hall force, or thermal force. As an example of the dynamic mobility, for simple harmonic vortex motion,  $\tilde{\mu}_v(\omega, B, T) = (-i\omega\mu + \eta + i\kappa_p/\omega)^{-1}$ , where  $\omega$  is the angular frequency and  $T$  the temperature. Generally  $\mu = \mu(T)$ ,  $\eta = \eta(B, T)$ , and the pinning force constant  $\kappa_p = \kappa_p(B, T)$ . It is typical at higher temperatures in the superconducting state for pinning to become weak, in which case  $\tilde{\mu}_v \rightarrow 1/\eta$ . The generalization of this to a tensor drag force is that the mobility approaches the inverse of the viscous drag tensor when pinning and inertia are negligible. From the mobility, the complex-valued resistivity associated with vortex motion follows from  $\tilde{\rho}_v = B\phi_0 \tilde{\mu}_v$ .

### MISALIGNED BANKS

We consider here a certain misalignment of the two superconducting banks, assuming the two banks are made of the same material. With the  $b$  axis common to both banks,

we consider two different angles  $\theta_i, i=1, 2$  of rotation of the  $a$  and  $c$  axes on the two junction sides. It turns out that the 1D sine-Gordon equation still governs the gauge invariant phase difference.<sup>8</sup> However, in order to describe that result we need to recall the pertinent effective mass tensors.

These are symmetric tensors  $m_{\alpha\beta}$  and  $\mu_{ij}$  given by

$$\begin{aligned} m_{xx} &= m_a \cos^2 \theta_i + m_c \sin^2 \theta_i, \\ m_{zz} &= m_a \sin^2 \theta_i + m_c \cos^2 \theta_i, \\ m_{xz} &= (m_c - m_a) \cos \theta_i \sin \theta_i, \quad m_{yy} = m_a, \end{aligned} \quad (10)$$

$$\begin{aligned} \mu_{xx} &= \frac{1}{\sqrt{m_a}} \cos^2 \theta_i + \frac{1}{\sqrt{m_c}} \sin^2 \theta_i, \\ \mu_{zz} &= \frac{1}{\sqrt{m_a}} \sin^2 \theta_i + \frac{1}{\sqrt{m_c}} \cos^2 \theta_i, \\ \mu_{xz} &= \left( \frac{1}{\sqrt{m_c}} - \frac{1}{\sqrt{m_a}} \right) \cos \theta_i \sin \theta_i. \end{aligned} \quad (11)$$

Then the appropriate sine-Gordon equation is<sup>8</sup>

$$\Lambda_{xx}^2 \varphi'' = \sin \varphi, \quad (12)$$

where

$$\Lambda_{xx}^2 = \lambda_J^2 \frac{2q_{xx}}{\det(q_{\alpha\beta})}. \quad (13)$$

The  $q_{\alpha\beta}$  tensor is given from Eqs. (10) and (11) by way of

$$q_{\mu\nu} = -e_{\mu\alpha} \{ m_{\alpha\beta} \mu_{\beta\gamma} \} e_{\gamma\nu}, \quad (14)$$

where  $e_{\mu\nu}$  is the 2D unit antisymmetric tensor defined by

$$\begin{aligned} e_{\mu\nu} &= 0 \quad \text{if } \mu = \nu \\ &= 1 \quad \text{if } \mu < \nu \\ &= -1 \quad \text{if } \mu > \nu. \end{aligned} \quad (15)$$

In Eq. (14),  $\{\cdot\cdot\cdot\}$  denotes the sum of a quantity taken on the two junction sides. In particular for Eq. (13), we note that

$$\begin{aligned} q_{xx} &= \{ m_{zx} \mu_{xz} + m_{zz} \mu_{zz} \} = \sqrt{m_a} (\sin^2 \theta_1 + \sin^2 \theta_2) \\ &\quad + \sqrt{m_c} (\cos^2 \theta_1 + \cos^2 \theta_2). \end{aligned} \quad (16)$$

Various explicit relations between the components of the tensors  $q_{\alpha\beta} = -e_{\alpha\gamma} p_{\gamma\beta}$  and  $p_{\gamma\beta}$  are recorded in the Appendix.

Similar to the calculations above, we can employ the single soliton solution  $\varphi(x) = 4 \tan^{-1}[\exp(x/\Lambda_{xx})]$  and obtain expressions for the drag coefficient and inertial mass per unit length in the nonrelativistic limit. The results are, respectively,

$$\eta(\theta_1, \theta_2) = \frac{2\phi_0^2}{\pi^2 c^2} \frac{1}{R'} \frac{1}{\Lambda_{xx}(\theta_1, \theta_2)}, \quad (17)$$

TABLE I. Summary of nonrelativistic calculations.

Quantity	Anisotropic banks			References
	Isotropic banks	Aligned	Misaligned	
$\mu$	$\frac{1}{2\pi^3} \frac{\phi_0^2}{\bar{c}^2 d\Lambda_J}$	$\frac{1}{2\pi^3} \frac{\phi_0^2}{\bar{c}^2 d\Lambda_J(\theta)}$	$\frac{1}{2\pi^3} \frac{\phi_0^2}{\bar{c}^2 d\Lambda_{xx}(\theta_1, \theta_2)}$	9, Eqs. (9), (18)
$\eta$	$\frac{2}{\pi^2} \frac{\phi_0^2}{c^2 R' \lambda_J}$	$\frac{2}{\pi^2} \frac{\phi_0^2}{c^2 R' \Lambda_J(\theta)}$	$\frac{2}{\pi^2} \frac{\phi_0^2}{c^2 R'_{xx}(\theta_1, \theta_2)}$	9, Eqs. (5), (17)
$H_{c1J}$	$\frac{2}{\pi^2} \frac{\phi_0}{d\Lambda_J}$	$\frac{2}{\pi^2} \frac{\phi_0}{d_b \Lambda_J(\theta)} \sqrt{\frac{k}{\cos^2 \gamma + k \sin^2 \gamma}}$		9, 10

$$\mu(\theta_1, \theta_2) = \frac{1}{2\pi^3} \frac{1}{\bar{c}^2} \frac{\phi_0^2}{d\Lambda_{xx}(\theta_1, \theta_2)}. \quad (18)$$

For the general situation of an arbitrary vortex orientation in the  $xz$  plane and misaligned banks, a 2D solution for the phase difference is required. The governing equation is<sup>8</sup>

$$\Lambda_{xx}^2 \frac{\partial^2 \varphi}{\partial x^2} + 2\Lambda_{xz}^2 \frac{\partial^2 \varphi}{\partial x \partial z} + \Lambda_{zz}^2 \frac{\partial^2 \varphi}{\partial z^2} = \sin \varphi, \quad (19)$$

where

$$\Lambda_{\alpha\beta}^2 = \lambda_J^2 \frac{2q_{\alpha\beta}}{\det(q_{\alpha\beta})}. \quad (20)$$

By a linear change of coordinates, the mixed derivative term  $\partial_x \partial_x \varphi$  can be eliminated. Then known solutions of the 2D sine-Gordon equation (e.g., Refs. 21 and 22) can be applied. It is also possible to directly find families of solutions of Eq. (19), but this idea is not pursued here.

The main results of the above nonrelativistic calculations are summarized in Table I. The right-most column gives the respective references for the entries of that row. The three isotropic results for the Josephson vortex mass per unit length, drag coefficient, and lower critical field are due to LS.<sup>9</sup> The numbers in parentheses in the fifth column refer to equations of this paper. The Mints result for the lower critical field of a junction with anisotropic but aligned banks<sup>10</sup> has been slightly extended with the introduction of the magnetic length in the  $b$  direction (perpendicular to the junction plane)  $d_b = 2\lambda_b + d_i$ . While in the isotropic case the vortex mass is directly proportional to the junction lower critical field,  $\mu = \phi_0 H_{c1J} / 4\pi \bar{c}^2$ , this no longer holds for anisotropic banks. For anisotropic but aligned banks, the angle  $\gamma$  such that  $\tan \gamma = (\tan \theta) / k$  gives the angle between the magnetic field  $\mathbf{H}$  and the  $c$  axis. In this case, the vortex axis  $\hat{z}$  and  $\mathbf{H}$  are not coincident directions. In fact, the angle  $\beta$  between these vectors is given by<sup>10</sup>

$$\tan \beta = - \frac{(k-1) \tan \theta}{k + \tan^2 \theta}. \quad (21)$$

### RELATIVISTIC CONSIDERATIONS

Here we describe the main ingredients of a relativistic calculation of the Josephson vortex mass and drag coefficient for the case of aligned banks. As seen in detail above, these results can be extended to the situation of misaligned banks

by making the replacement  $\Lambda_J(\theta) \rightarrow \Lambda_{xx}(\theta_1, \theta_2)$ . This is possible because the 1D sine-Gordon equation still governs the space-time evolution of the phase difference.

The time-dependent extension of Eq. (1) is

$$\Lambda_J^2 \varphi'' - \omega_J^{-2} \ddot{\varphi} = \sin \varphi, \quad (22)$$

where  $\dot{\phantom{x}}$  denotes differentiation with respect to time and  $\omega_J \equiv \bar{c} / \Lambda_J$ . We are now interested in the covariant single soliton solution

$$\varphi(x, t) = 4 \tan^{-1} [\exp \gamma_v (x - vt) / \Lambda_J], \quad (23)$$

where  $\gamma_v \equiv \sqrt{1 - v^2 / \bar{c}^2}$ , which exhibits Lorentz contraction.

We simplify the calculation of  $\mu$  and  $\eta$  by ignoring the production of radiation. This phenomenon has been treated in Ref. 23 by means of a Green's-function approach. In any experimental situation where relativistic Josephson vortex velocities are approached, there will be an acceleration stage when radiation will occur. Similarly, whenever a vortex decelerates from relativistic to low speeds there is radiation, which is specifically outside the scope of the present treatment.

In calculating the electromagnetic contribution to the vortex mass per unit length, we put the relativistic kinetic energy  $K = (\gamma_v - 1) \mu \bar{c}^2$  equal to the electric-field energy:

$$(\gamma_v - 1) \mu \bar{c}^2 = \frac{\epsilon}{8\pi} \int E^2(\mathbf{x}) d^2 x. \quad (24)$$

Assuming that the relation between the electric-field component across the junction  $E_y$  and  $\varphi$  holds as before, and carrying out Eq. (24) with the vortex solution (23) yields a velocity-dependent mass per unit length,

$$\mu(\theta, v) = \frac{1}{4\pi^3} \frac{1}{\bar{c}^4} \frac{\phi_0^2}{d\Lambda_J(\theta)} \frac{\gamma_v v^2}{(\gamma_v - 1)}. \quad (25)$$

As  $v \rightarrow 0$ , this becomes the nonrelativistic result (9).

In special relativity, the velocity  $\mathbf{v}$  is not the spatial part of a four vector, but  $\gamma_v \mathbf{v}$  is, which is a reflection of the fact that time and proper time  $\tau$  are related by  $\partial t / \partial \tau = \gamma_v$ . In addition, the Newtonian force  $F_i$  is related to the Minkowski force  $K_i$  by a factor of  $\gamma_v$ ,  $F_i = K_i / \gamma_v$ . Therefore it appears that the scalar power dissipation  $\mathbf{F} \cdot \mathbf{v}$  is unchanged from  $\eta v^2$  when the drag force is  $-\eta \mathbf{v}$ . This result may be particular to this form of the drag force.



Taking  $\eta v^2$  as the dissipated power, we can then straightforwardly use the covariant solution (23) in Eq. (4), with the result

$$\eta(\theta, v) = \frac{2\phi_0^2}{\pi^2 c^2} \frac{1}{R'} \frac{\gamma_v}{\Lambda_J(\theta)}. \quad (26)$$

This expression has a relatively simple dependence upon velocity, reducing to Eq. (5) when  $v \rightarrow 0$ . As  $v$  approaches  $\bar{c}$ , the drag coefficient becomes infinite which appears qualitatively acceptable. As mentioned above, our simple approach breaks down when the dissipation becomes sufficiently large. When  $v$  becomes comparable to  $\bar{c}$  the sine-Gordon equation should be modified to explicitly incorporate the effect of the frictional force and then an improved approach to finding the power dissipated is called for.

We conclude this section by indicating how the mass per unit length and drag coefficient can be computed for a 1D array of Josephson vortices. In this case, the appropriate phase difference solution of Eq. (22) is

$$\varphi(x, t) = 2 \sin^{-1} \{ \text{sn} [ \gamma_v (x - vt) / k \Lambda_J ] \} + \pi, \quad (27)$$

where  $0 \leq k \leq 1$  is the modulus of the Jacobi elliptic function sn. Since the magnetic-field component  $H_z$  varies as  $\partial\varphi/\partial x$  and the function dn  $u$  has real period  $2K(k)$ ,  $2(\Lambda_J/\gamma_v)kK(k)$  is the distance between adjacent vortices. Here,  $K(k)$  is the complete elliptic integral of the first kind. In Eq. (27), the function sn oscillates between  $-1$  and  $1$ . When the modulus  $k \rightarrow 1$ ,  $K(k) \rightarrow \infty$ , and we have the weak-field limit. In this limit, sn can be approximated by  $\tanh$ .<sup>24</sup> On the other hand, for  $k \rightarrow 0$ ,  $K(0) = \pi/2$  and we have the strong-field limit.

By using the relations  $1 - \text{sn}^2 u = \text{cn}^2 u$ ,  $d \text{sn} u / du = \text{cn} u \text{dn} u$ , and  $\int_0^u \text{dn}^2 w dw = E(u|m)$  between Jacobi elliptic functions we can apply Eq. (4) to the solution (27) to give

$$\eta(\theta, v) = \frac{2\phi_0^2}{\pi^2 c^2} \frac{1}{R'} \frac{E(k)}{k} \frac{\gamma_v}{\Lambda_J(\theta)}, \quad (28)$$

where  $E(k)$  is the complete elliptic integral of the second kind. This result is larger than the relativistic result (26) for a single vortex by the factor  $E(k)/k$ . We have  $E(0) = \pi/2$  and  $E(1) = 1$ , so that Eq. (26) is properly recovered in the weak-field limit.

Similarly, applying Eq. (27) in Eq. (24) we find for the mass per unit length of a 1D Josephson vortex array moving uniformly in the junction barrier

$$\mu(\theta, v) = \frac{1}{4\pi^3} \frac{1}{\bar{c}^4} \frac{E(k)}{k} \frac{\phi_0^2}{d\Lambda_J(\theta)} \frac{\gamma_v v^2}{(\gamma_v - 1)}. \quad (29)$$

This electromagnetic contribution to the vortex mass is increased over Eq. (25) by the factor  $E(k)/k$ .

### SUMMARY

In summary, the mass per unit length  $\mu$  and drag coefficient  $\eta$  for a Josephson vortex moving and aligned parallel to the plane of an anisotropic Josephson junction have been derived. The anisotropy of the superconducting banks is described by effective mass tensors, Eqs. (10) and (11). In these equations, the tilt angles  $\theta_i$  between the vortex direc-

tion  $\hat{z}$  and the crystal uniaxial directions ( $\hat{c}$ ) of the banks are parameters, so that a simple misalignment of the banks is included.

Results have been presented for both the nonrelativistic and relativistic limits of vortex motion. For junctions made of barriers with large dielectric constant and superconducting banks with large penetration depth, the latter regime begins at lower vortex speeds. The nonrelativistic results are encapsulated in Table I, while Eqs. (23)–(29) are relevant to the relativistic treatment.

The low magnetic-field results obtained here can be used in the vortex dynamic mobility. Applications of this function include the description of the microwave response of Josephson vortices. In particular, the drag coefficient is needed to characterize the energy dissipation due to vortex motion and thus impacts the surface resistance. Relevant to radio frequency response may then be Eqs. (5) and (17) for single vortices and Eq. (28) for a 1D array of vortices.

The description developed here should be applicable to the polycrystalline nature of many samples of high- $T_c$  superconductors. In particular, when vortices first penetrate along twin planes, they are expected to be of the Josephson type. The present approach should be applicable to either the motion of Josephson vortices along twin boundaries or the intergrain motion in granular samples.

### APPENDIX

Here we explicitly evaluate the tensors  $p_{\alpha\beta}(\theta_1, \theta_2)$  and  $q_{\alpha\beta}(\theta_1, \theta_2)$  by using Eqs. (10)–(11) and (14)–(15). This supplies many useful relations for the case of misaligned superconducting banks. From the tensor  $p_{\alpha\beta}$  we have the components of the magnetic field  $H_\alpha$ ,  $\alpha = x, z$  in terms of the gauge invariant phase difference  $\varphi$  as

$$H_x(x) = \frac{p_{zz}}{|p_{\alpha\beta}|} \frac{\phi_0}{2\pi\lambda} \varphi'(x), \quad (A1)$$

$$H_z(x) = -\frac{p_{zx}}{|p_{\alpha\beta}|} \frac{\phi_0}{2\pi\lambda} \varphi'(x), \quad (A2)$$

where  $'$  denotes differentiation with respect to  $x$  and  $|\dots|$  denotes determinant.

For the tensor

$$p_{\alpha\beta} = \begin{bmatrix} p_{xx} & p_{xz} \\ p_{zx} & p_{zz} \end{bmatrix} \quad (A3a)$$

we find that

$$p_{xx} = -(\sqrt{m_c} - \sqrt{m_a})(\sin \theta_1 \cos \theta_1 + \sin \theta_2 \cos \theta_2), \quad (A3b)$$

$$p_{xz} = \sqrt{m_a}(\cos^2 \theta_1 + \cos^2 \theta_2) + \sqrt{m_c}(\sin^2 \theta_1 + \sin^2 \theta_2), \quad (A3c)$$

$$p_{zx} = -\sqrt{m_a}(\sin^2 \theta_1 + \sin^2 \theta_2) - \sqrt{m_c}(\cos^2 \theta_1 + \cos^2 \theta_2), \quad (A3d)$$

$$p_{zz} = -p_{xx}. \quad (A3e)$$

For use in equations such as Eqs. (A1) and (A2) we have the determinant

$$|p_{\alpha\beta}| = (m_a + m_c)[1 - (s_1 s_2 + c_1 c_2)^2] + \sqrt{m_a m_c}[2(s_1 c_1 + s_2 c_2)^2 + (s_1^2 + s_2^2)^2 + (c_1^2 + c_2^2)^2], \quad (\text{A4})$$

where  $s_i \equiv \sin \theta_i, c_i \equiv \cos \theta_i, i = 1, 2$ . When the aligned but anisotropic banks case holds,  $\theta_1 = \theta_2 = \theta$ , Eq. (A.4) properly

gives  $4\sqrt{m_a m_c}$ . In regard to Eq. (13), we have  $|q_{\mu\nu}| = |p_{\alpha\nu}|$  because  $|-e_{\mu\alpha}| = 1$ . Since

$$\begin{bmatrix} q_{xx} & q_{xz} \\ q_{zx} & q_{zz} \end{bmatrix} = \begin{bmatrix} -p_{zx} & -p_{zz} \\ p_{xx} & p_{xz} \end{bmatrix}, \quad (\text{A5})$$

the squared lengths  $\Lambda_{\alpha\beta}^2(\theta_1, \theta_2)$  of Eq. (20) are explicitly determined.

- 
- <sup>1</sup>N.-C. Yeh, Phys. Rev. B **43**, 523 (1991).  
<sup>2</sup>M. W. Coffey and J. R. Clem, Phys. Rev. Lett. **67**, 386 (1991).  
<sup>3</sup>G. Blatter, V. B. Geshkenbein, and V. M. Vinokur, Phys. Rev. Lett. **66**, 3297 (1991).  
<sup>4</sup>M. W. Coffey and J. R. Clem, Phys. Rev. B **44**, 6903 (1991).  
<sup>5</sup>M. W. Coffey and J. R. Clem, Phys. Rev. B **48**, 342 (1993).  
<sup>6</sup>Z. Hao and J. R. Clem, IEEE Trans. Magn. **MAG-27**, 1086 (1991).  
<sup>7</sup>M. W. Coffey and Z. Hao, Phys. Rev. B **44**, 5230 (1991).  
<sup>8</sup>R. G. Mints and V. G. Kogan, Phys. Rev. B **60**, 1394 (1999).  
<sup>9</sup>P. Lebowitz and M. J. Stephen, Phys. Rev. **163**, 376 (1967).  
<sup>10</sup>R. G. Mints, Mod. Phys. Lett. B **3**, 51 (1989).  
<sup>11</sup>M. W. Coffey, J. Phys. A **31**, 6103 (1998).  
<sup>12</sup>J. U. Lee, J. E. Nordman, and G. Hohenwarter, Appl. Phys. Lett. **67**, 1471 (1995); J. U. Lee and J. E. Nordman, Physica C **277**, 7 (1997); J. U. Lee *et al.*, Appl. Phys. Lett. **71**, 1412 (1997).  
<sup>13</sup>J. R. Clem and M. W. Coffey, Phys. Rev. B **42**, 6209 (1990).  
<sup>14</sup>J. McDonald and J. R. Clem, Phys. Rev. B **56**, 14 723 (1997).  
<sup>15</sup>M. B. Gaifullin *et al.*, Phys. Rev. Lett. **83**, 3928 (1999); **81**, 3551 (1998).  
<sup>16</sup>T. Shibauchi *et al.*, Phys. Rev. Lett. **83**, 1010 (1999).  
<sup>17</sup>E. B. Sonin, Phys. Rev. Lett. **79**, 3732 (1997); **81**, 3552 (1998).  
<sup>18</sup>H. Enriquez, Y. De Wilde, N. Bontemps, and T. Tamegai, Phys. Rev. B **58**, R14 745 (1998).  
<sup>19</sup>T. Shibauchi *et al.*, Phys. Rev. B **57**, R5622 (1998).  
<sup>20</sup>K. K. Likharev, *Dynamics of Josephson Junctions and Circuits* (Gordon and Breach Science, New York, 1986).  
<sup>21</sup>G. Leibbrandt, Phys. Rev. B **15**, 3353 (1977); S. I. Ben-Abram, Phys. Lett. A **55**, 383 (1976).  
<sup>22</sup>J. Zagrodzinski, Phys. Lett. **57A**, 213 (1977); **72A**, 284 (1979).  
<sup>23</sup>D. W. McLaughlin and A. C. Scott, Phys. Rev. A **18**, 1652 (1978).  
<sup>24</sup>I. S. Gradshteyn and I. M. Ryzhik, *Table of Integrals, Series, and Products* (Academic, New York, 1980); *Handbook of Mathematical Functions with Formulas, Graphs, and Mathematical Tables*, edited by M. Abramowitz and I. A. Stegun, Natl. Bur. Stand. Appl. Math. Ser. No. 55 (U.S. GPO, Washington, D.C., 1972).